THE SUN, THE OCEAN AND CO_2 : AN OBJECTIVE APPROACH TO THE SOLAR ENERGY CONTRIBUTION

Brigitte Van Vliet-Lanoë, emeritus senior CNRS scientist

Dec 27, 2024

We live on a **blue planet**, whose main characteristic is the presence of an ocean responsible for 70% of the energy stored by the sun**. The mass of the Earth's oceans is 300 times that of the atmosphere, and its thermal storage capacity is 1,000 times higher that of the atmosphere**. The ocean therefore acts as a planet's thermal regulator, since it has greater thermal inertia than the atmosphere. Given the presence of the ocean (Figure 1), our planet has an atmosphere rich in water vapour and therefore variable cloud cover. Atmospheric water vapour, the main greenhouse gas, plays a major role in the Earth's radiative balance by absorbing incoming (solar) infrared radiation and outgoing IR radiation re-emitted at the planet's surface.

A recent analysis by Nikolov and Zeller (2024) revealed that the observed decrease in global albedo (cloud cover and ice) and measured variations in total solar irradiance (TSI) alone explain 100% of the direct global warming trend and 83% of the interannual variability in Global Surface Air Temperature (GSAT) over the last 24 years of satellite and ground-based thermal measurements. According to these authors, changes in the albedo of terrestrial clouds are the dominant factor in changes in tropospheric temperature, while the TSI plays only a marginal role. **This overlooks the role of thermal storage in the upper intertropical ocean.**

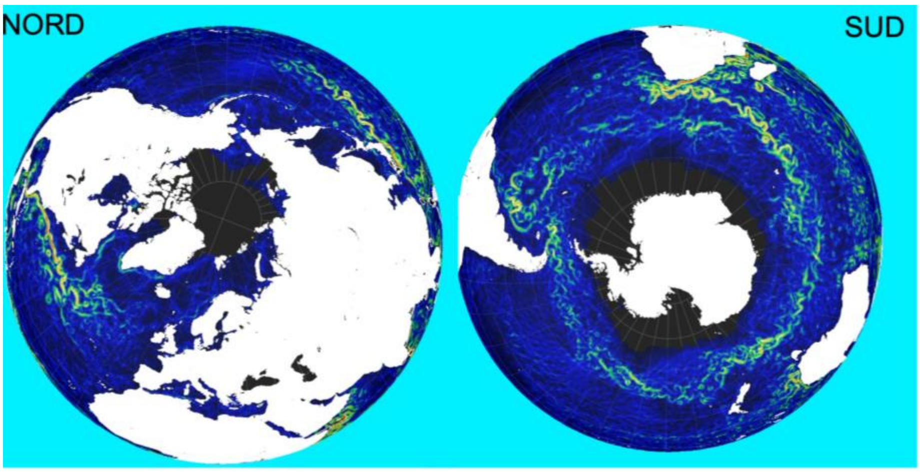

Figure 1. 62% of the Northern Hemisphere (NH) is covered by water with the Arctic Ocean, while 82% of the Southern Hemisphere (SH) is covered by water with the Antarctic Circumpolar Ocean.

Another factor, albeit transitory, is directly related to the sudden stratospheric warming associated with solar flares (SCE, 2024), more specifically in the NH polar vortex, much infrequent in the SH, in connection with eruptive solar activity and the destruction of ozone in the lower stratosphere.

Nevertheless, for us, **the ocean is the cumulative radiator of the energy received by our planet, re-emitting most of the planetary IR, with cloud cover acting as a buffer for the energy re-emitted to space. The presence of water and vapour emitted are the 2 factors responsible for the indirect heating of our atmosphere by the energy emitted towards our planet by a variable sun.**

1. HOW TO WARM THE OCEAN SURFACE?

The thermal structure and composition of our atmosphere are fundamentally determined by incoming solar radiation. UV radiation dissociates ozone and is the main source of heat for the lower stratosphere, while visible and infrared radiation mainly reaches and warms the lower troposphere and the Earth's surface, including the ocean. The spectral composition of solar radiation is therefore crucial in determining atmospheric structure (Haigh et al. 2010).

However, this does not consider the penetration of solar energy through 100 km of troposphere into the ocean. This penetration is limited to the visible part of sunlight and the near UV (short wavelengths) which transfer their energy below the ocean surface. If we apply Beer-Lambert's law (SCE, 2024) blue light can penetrate to a depth of 245 m, while red light can only penetrate to a depth of 2.6 metres. **Mid- and far-infrared light can only penetrate the surface of seawater to a depth of around 20 microns!**

To explain this, we need to understand **how the intertropical ocean, which receives the most energy, heats up and re-emits a large amount of IR energy into the atmosphere through dynamic evaporation at its surface. It is the planetary radiator: solar radiation absorbed through the surface layer of the oceans (~250 m) is the main source of IR energy for our climate system.**

However, the ocean is not a black body: the IR received at its surface nevertheless contributes to the strong dynamic evaporation at the ocean surface.

As a result, heating of the ocean mass is greatest between the 2 tropics, where insolation is almost orthogonal to the planet and therefore optimal. Nearly 99% of the energy absorbed is in the short wavelength range from 0.3 to 3 μm (UVA, UVB and visible), including the blue. Although highly filtered by the ozone layer, solar ultraviolet (UVB and UVA) penetrates seawater to a depth of -250 m, the frequent position of the thermocline (Figure 2). **This absorption will cumulatively warm the intertropical ocean at this depth, where insolation is at its highest depending on the season, i.e. just below the thermal equator, and therefore constrains the depth of the thermocline. Its thermal absorption is often attenuated depending on the particle or plankton load of the sea and, above all, the variable tropospheric cloud cover.** According to the IPCC, it only penetrated the ocean with an average energy of around 16 mW/cm^2, i.e. slightly more than one tenth of the initial solar radiation, which seems insufficient to explain the temperatures reached (>30°C in the Philippines or the Red Sea).

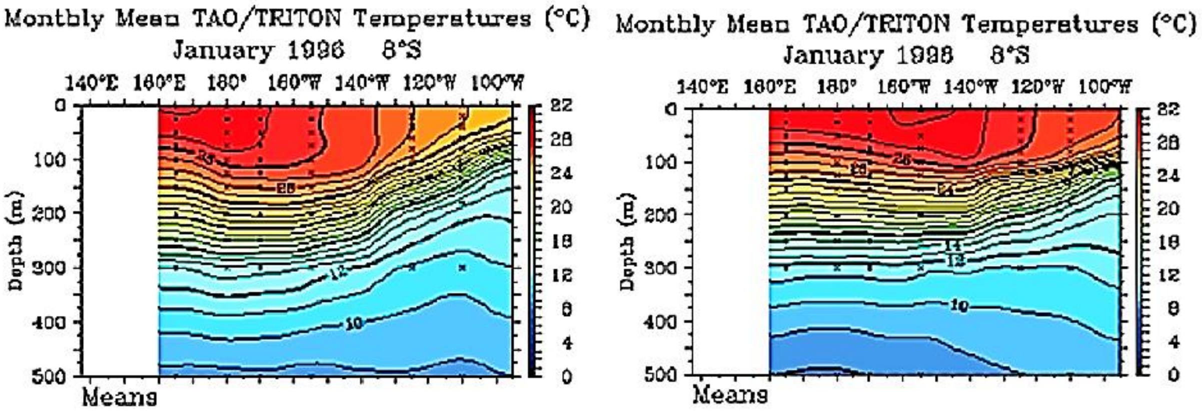

Figure 2. Position of the thermocline during an El Niño (January 1996, left) and an El Niña (January 1998, right) from data collected by Argos drifting buoys ([Thermocline]() thick black line

2. IMPACT OF ORBITAL FORCING

The orbital forcing of our interglacial, the Holocene, is like that of the previous interglacial, the Eemian (133-113 ka BP). It shows two 2 millennial thermal maxima in the Southern Hemisphere, and one minimum corresponding to the Northern Hemisphere maximum (Fig.3). The trends are identical but less intense for the Holocene. For the HN, this forcing implies 3 thermal maxima :

- The one that triggered the last deglaciation 21 ka BP ago, under the influence of HS insolation.
- The Holocene thermal optimum corresponds to the peak of insolation in the HN, 7890 years ago BP.
- **and the 3rd, which began 3,650 BP ago, under the influence of a maximum in the HS and which we are still in.**

We are currently at the end of an interglacial, a maximum of solar activity initiated 3.6 ka BP ago by orbital forcing in the Southern Hemisphere (SH). It is recorded by heat storage in the intertropical ocean and transmitted to the NH by the thermohaline circulation, alias the Gulf Stream and the North Atlantic drift, and, associated in addition to marked solar events (^{14}C and 30 beryllium) marked **by powerful Niño events. So since 3.6 ka we have been in a slow cooling phase, pulsed by a series of optima of decreasing intensity** (Minoan, Roman, Middle Ages and present day). These are separated from the HN optimum (8 ka BP) by the cooling of the Subboreal, around 5 ka BP ago. The present-day optimum is a direct descendant of the previous ones. A similar situation occurred during the previous interglacial (133-113 ka BP), with the disappearance of the Icelandic cap and a second eustatic maximum between 116 and113 ka (Frontval et al., 1998 ; Van Vliet-Lanoë 2018, - et al 2018).

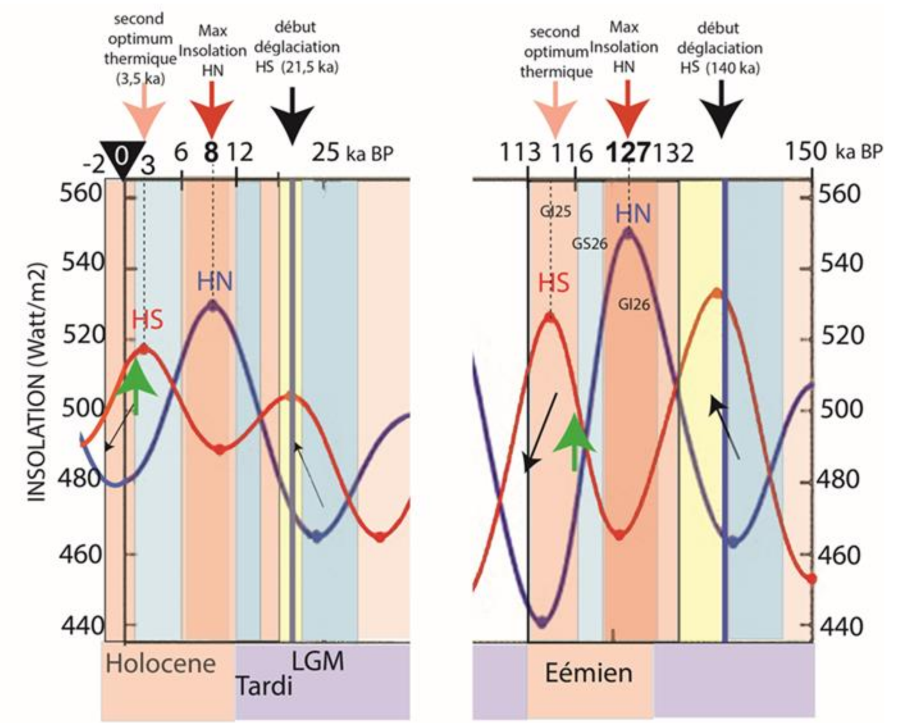

Figure 3. Comparative changes in total insolation in the southern and northern hemispheres during the Holocene and Eemian (at 65° north and south; 20). Thermal evolution of the Northern Hemisphere, Van Vliet-Lanoë, 201).

3. IMPACT OF SOLAR ACTIVITY

Our Sun is a variable star 30,000 times bigger than the Earth. The core of the Sun's mass is responsible for 98% of the energy produced by nuclear fusion. It occurs in the form of electromagnetic radiation (gamma photons), where the density and temperature of the star are highest. The photons created in this very high-density environment interact repeatedly with the particles in the solar plasma, transferring energy to them. As a result, these photons lose energy and increase their wavelength, reaching the photosphere as visible light and escaping into interplanetary space. The balance between external gravitational forces (linked to the multiple interactions of the Sun, Jupiter and Pluto: Le Mouel et al., 2023) and pressure forces maintains the nuclear furnace in hydrostatic equilibrium. An increase in the fusion rate (confinement) will raise the temperature and the core will expand (Strong et al., 2012). An expansion of the core will reduce its density and slow the rate of the fusion reaction. **So, when the sun expands, the light and particle energy emitted by the star will decrease and its luminous intensity will fall. Conversely, when the Sun contracts, it will emit lighter and therefore more energy towards space and the Earth.**

Nearly 5% of the Sun's electromagnetic energy is emitted in the form of UV radiation. UV irradiance can vary from 10 to 40% over the course of a Schwabe cycle. When the Sun is at the maximum of the Schwabe cycle, a 1-10% increase in UV light emission has been measured (Ermolli, et al. 2013). Particles arrive via the solar wind: mainly protons (hydrogen nuclei), with around 10% alpha particles (helium nuclei) and traces of heavy ions (carbon, nitrogen, oxygen, silicon, iron, magnesium, etc.).

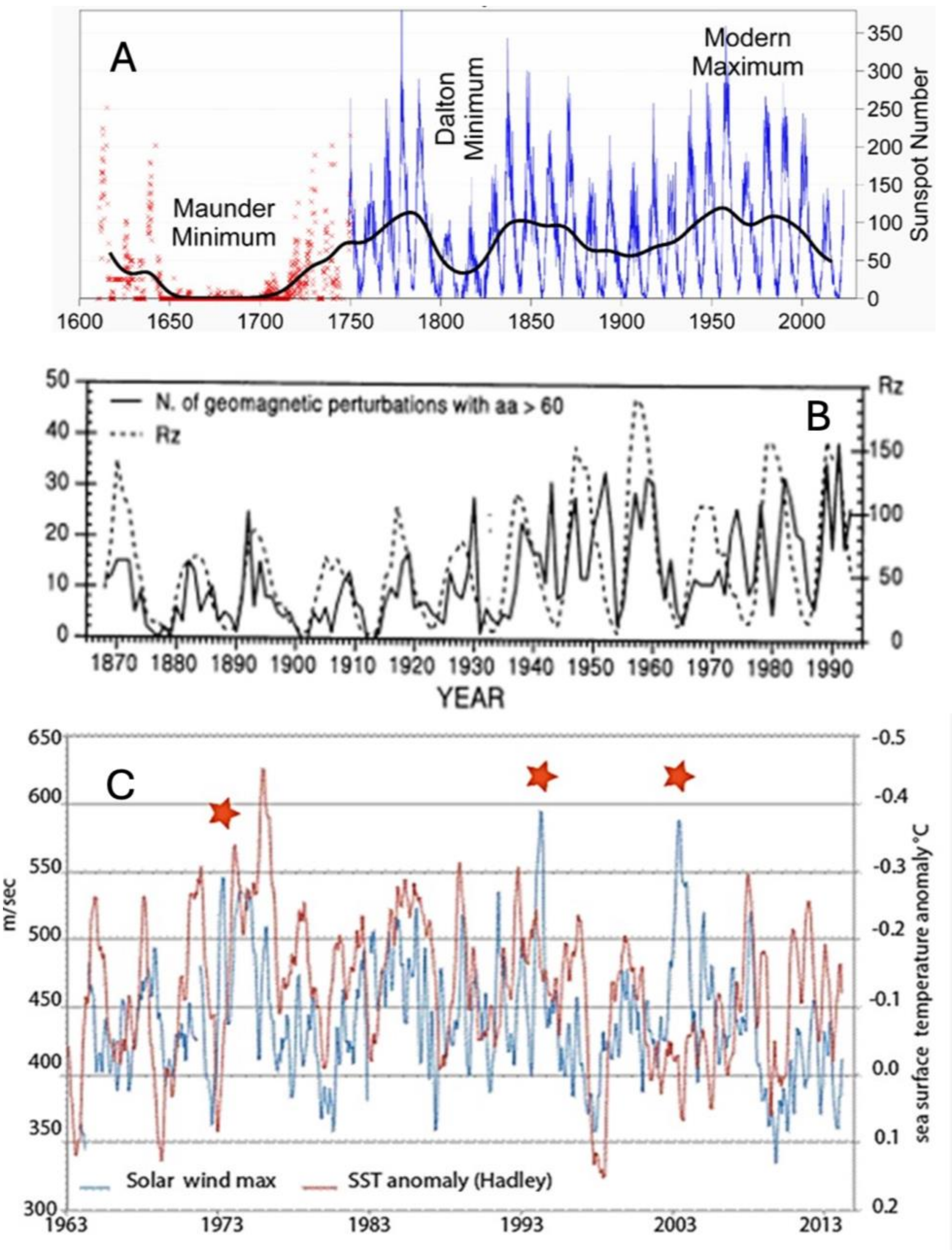

*Figure 4. **A**) Evolution of the increasing intensity of solar activity since the Maunder Minimum (Schwabe cycles, via the number of sunspots) **B**) Number of intense geomagnetic storms associated with coronal mass ejections (aa > 60) compared with the 11-year solar cycles (Storini, 1998). **C**) Comparative graph of the evolution of the energetic solar wind (blue, in km/sec) and sea surface temperature (red) since 1963. The red stars (heatwaves) are under the control of the solar wind. https://notrickszone.com/2014/05/22/data-suggest-that-solar-wind-impacts-global-temperature/).*

During periods of low activity, the particles are ejected at a speed of around 500 km/sec. In the event of a solar flare, the wind speed can exceed 1000 km/s (May, 2024: 1200 km/s). During the Maunder solar minimum (between 1645 and 1715), a global reduction of 50% in the strength of the heliospheric magnetic field and in the speed of the solar wind has been evaluated using various proxies (Owens et al., 2017) in the vicinity of the Earth.

During active periods, a strong solar wind formed by plasma can bring a lot of energy to the surface of the ocean (Figure 4C). The measured intensity of UV A and B radiation at latitudes below 50° north and south increased by 10-20% overall between 1996 and 2020, but much more over the South Pole (Bernhard et al., 2023; Xie et al., 2023), reflecting a gradual increase in the solar energy emitted over the last quarter of a century. The intensity of Schwabe cycles has been gradually increasing since the Maunder Minimum, but the preceding warm episode is linked to a peak in solar activity from 1320 to 1380 AD, leading to the end of the medieval optimum (officially 1350 AD), now considered to be a powerful Dansgaard-Oeshger event in the HN (Lapointe and Bradley, 2021).

During the sun's active phases, moderately energetic UV radiation (A and B) is absorbed by the intertropical ocean, resulting in heating that is effective over a few tens of metres and, consequently, complements direct surface evaporation via accumulated latent heat and heat transfer from the ocean to the troposphere and even the lower stratosphere. This absorption by the ocean is exacerbated by the action of high amplitude swells, winds (such as cyclones) and current vortices that stir up the surface water and redistribute this heat deep down into a surface layer around 200 metres thick, the thermocline. Its thickness can be modified by the action of the prevailing winds, as in the case of the trade winds in the intertropical zone or the westerly winds around 50° N.

Finally, the sun's magnetic field, which is strengthened by coronal mass ejections (CMEs), is responsible for a reduction in cloud cover by repelling the "cosmic" rays (solar and cosmic rays; charged particles: mainly protons and helium nuclei) responsible for the nucleation of water droplets.

4. ATMOSPHERIC CIRCULATION IN THE INTERTROPICAL ZONE

Because of the 23.5° tilt of the Earth's axis of rotation, the Sun in the tropics is never more than a few degrees (max 23.5°) from the zenith at midday throughout the year. This provides maximum energy on either side of the geographical equator, whether at sea or on land. Given the superficial absorption of energy by land formations, their warming is very limited, particularly given the high albedo of dry land (see Sahara). Intertropical rainforests, on the other hand, function almost like a black body, considering photosynthesis and evapotranspiration, but are often masked by cloud cover linked to the evapotranspiration of plants. Finally, over the ocean, saturation vapour pressure increases by 20% for every 3°C rise in water temperature, which amplifies cloudiness and convective instability.

4.1. THE TRADE WINDS AND THE EARTH'S ROTATION SPEED (DAY LENGTH)

Several factors control the zonal strength of the trade winds in the inter-tropical zone. The variability of the Earth's rotation speed is managed by the gravitational torque exerted by the Moon, the Sun and the planets. Classically considered to be stable, the variation in the Sun's diameter (see §3) causes a variation in the solar constant. When solar activity is low (quiet sun), the Sun's diameter increases, as it did during the Maunder Minimum, the speed of the solar wind decreased, and the speed of the Earth's rotation slows by 3% compared with today. The trade winds were powerful (between 1645 and 1715, maritime colonisation).

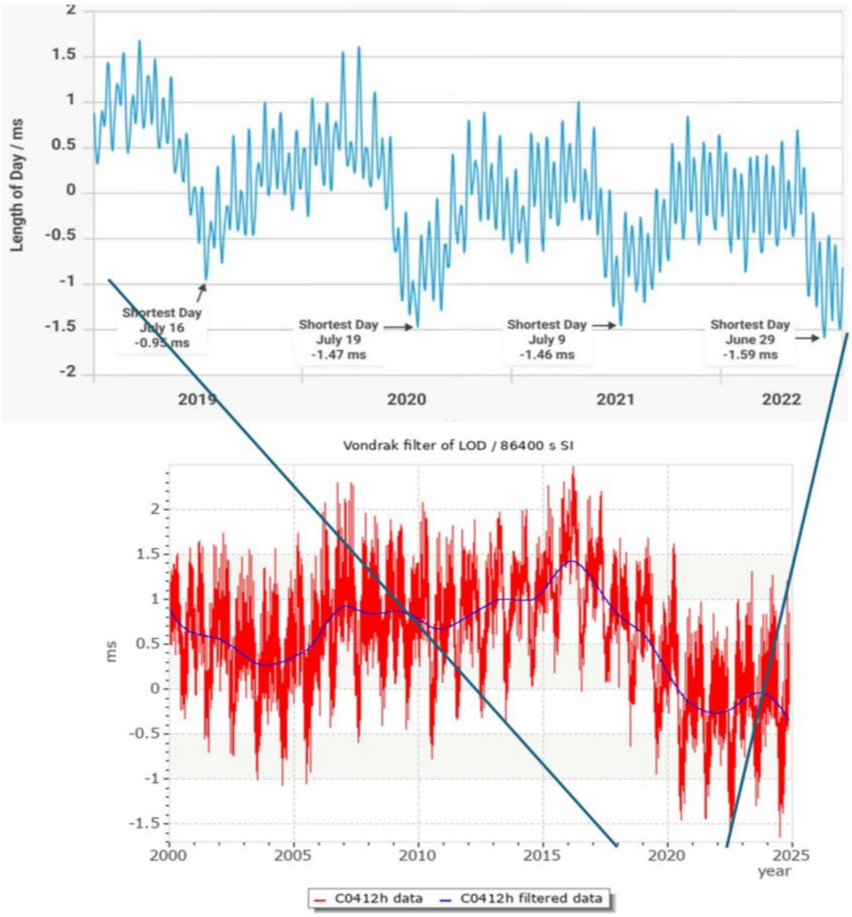

*Figure 5. **A**) Slowing of the Earth's rotation speed as indicated by the length of day (LOD). https://www.timeanddate.com/news/astronomy/shortest-day-2022 **B**) On the same vertical scale, long-term slowing of the Earth's rotation speed for the period 2000-2025. Note the very clear slowdown in LOD with solar maximum 2021-24. Images Bizouard, IERS EOP PC Observatoire Paris.*

The speed of the Earth's rotation has been falling from 1830 to 2020. Since 2020 (the start of measurements in the 1970s), rotation has accelerated with the Sun's increasing activity (Figure 5), reaching 1,670 km/h in 2024 instead of 1,600 km/h at the equator in 2020. At the pole, it is only about 3 km/h. When its diameter shrinks during periods of high activity, the trade winds slow down.

The Earth's rotation generates a tangential force of inertia, the Coriolis force, which will distort the trajectory of the winds in the lower troposphere. This force is zero at the equator, weak around 30° latitude, but sufficient to create a westward deviation in the circulation, creating the trade winds (north-easterly in the northern hemisphere and south-easterly in the southern hemisphere). The ocean, which stores heat during periods of strong solar activity, leads to a deep warming of the waters and weaker trade winds. It should be noted that in 2023, a year of exceptional solar activity, the trade winds were slowed to less than 20 km/h during the El Niño period (Fig.6). This year (2024), the speed of the trade winds exceeded 45 km, heralding a meteo-climatic cooling.

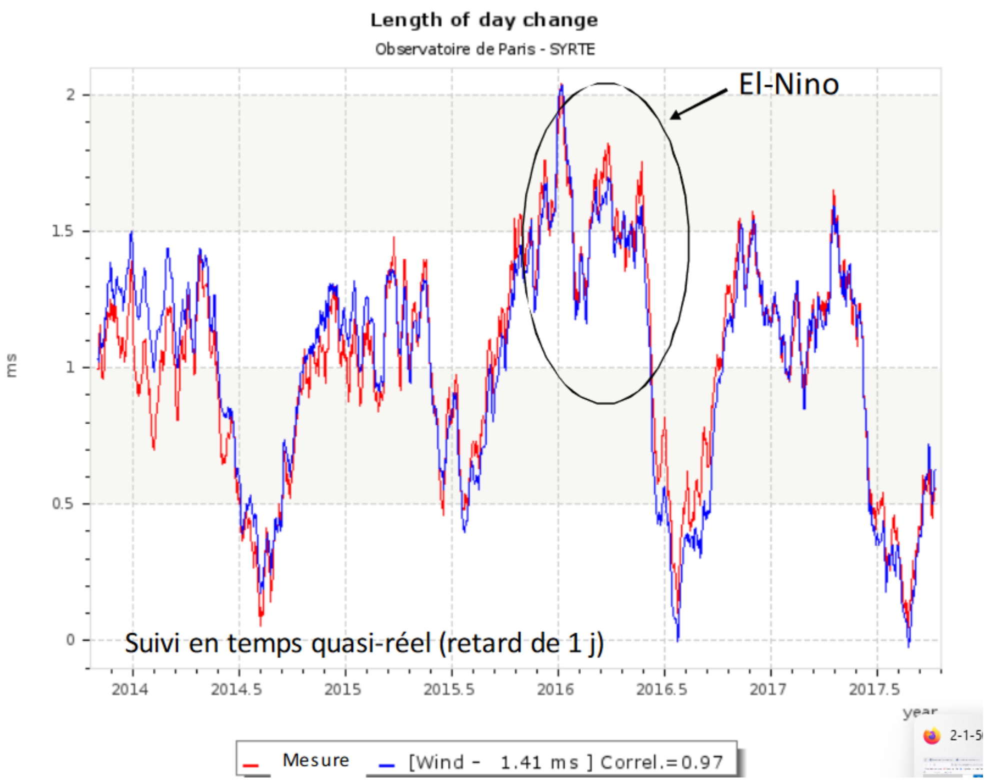

Figure 6. Length of day: (sub)seasonal variation like the effect of trade winds on El-Nino during periods of high solar activity (Bizouard, 2017) Length of day: modulation in 11.8 years of the semi-Annual component.

4.2. THE TRADE WINDS

The trade winds blow steadily from east to west in the lower troposphere, from subtropical high pressure (subtropical ridge of high pressure in the tropics) towards equatorial low pressure, the ICTZ (Intertropical Convergence Zone). They are active at altitudes of up to 5,000m, relayed in the upper troposphere by a very fast jet stream moving in the opposite direction. The position of the ICTZ varies according to the season. It is correlated with the Thermal Equator. This is the origin of the large convective structures on either side of the equator, the Hadley cells, which rise in altitude on either side of the thermal equator to an altitude of at least 30 km, forming in the upper troposphere a powerful "wall of westerly winds" (tropical jet stream) still perceptible in the lower stratosphere (75 km/h in mid-November, 125 km/h on 15 December; Figure 7). This 'wall' may act as a barrier to the tropospheric dynamics of CO_2, and in the equatorial stratosphere, there is some turbulence between the 2 tropical (N & S) jet streams in the lower stratosphere. Between 1965 and 2007, the lower stratosphere underwent considerable cooling (0.5 to 0.6 K/decade) in relation to a reduction in the lower stratospheric ozone layer, destroyed by the increase in solar UVC and an increase in water vapour content, attesting to increasing solar activity. It should be noted that the stratospheric and mesospheric water vapour content detected since less than 1980 could contribute significantly to the cooling of the global lower stratosphere (Ramaswamy and 2021).

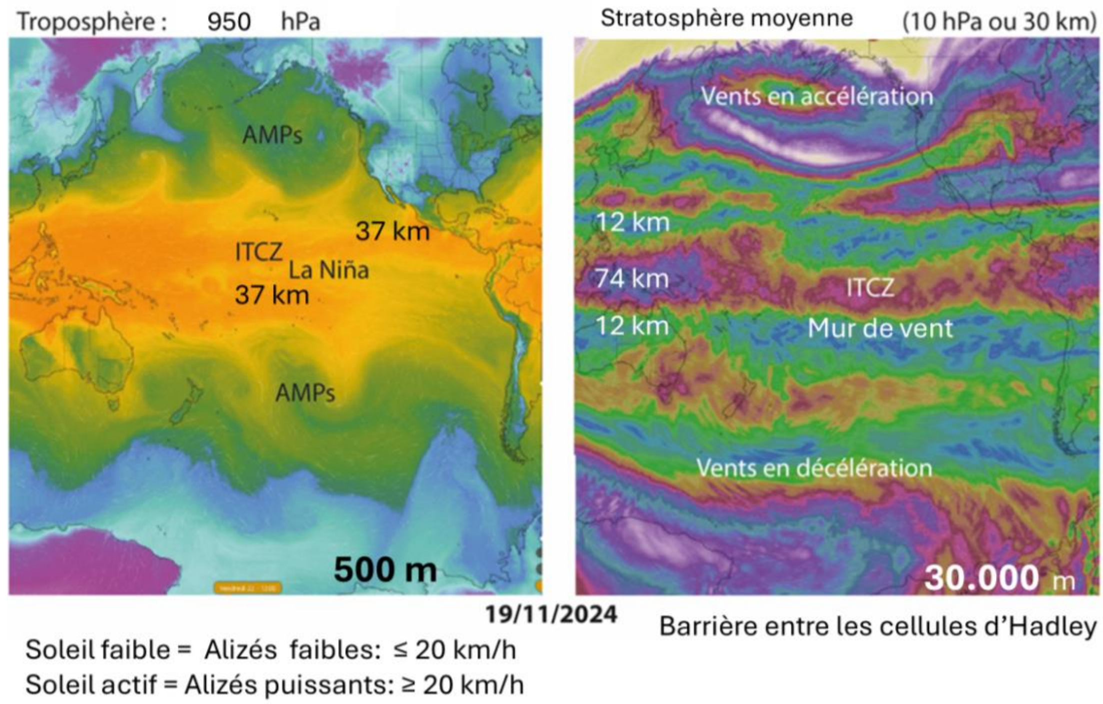

Figure 7. Air temperature and easterly wind speeds (trade winds) at 500 and 30,000m altitude (stratospheric jets). Note the wall of convective easterly winds in 2024 above the ITCZ.

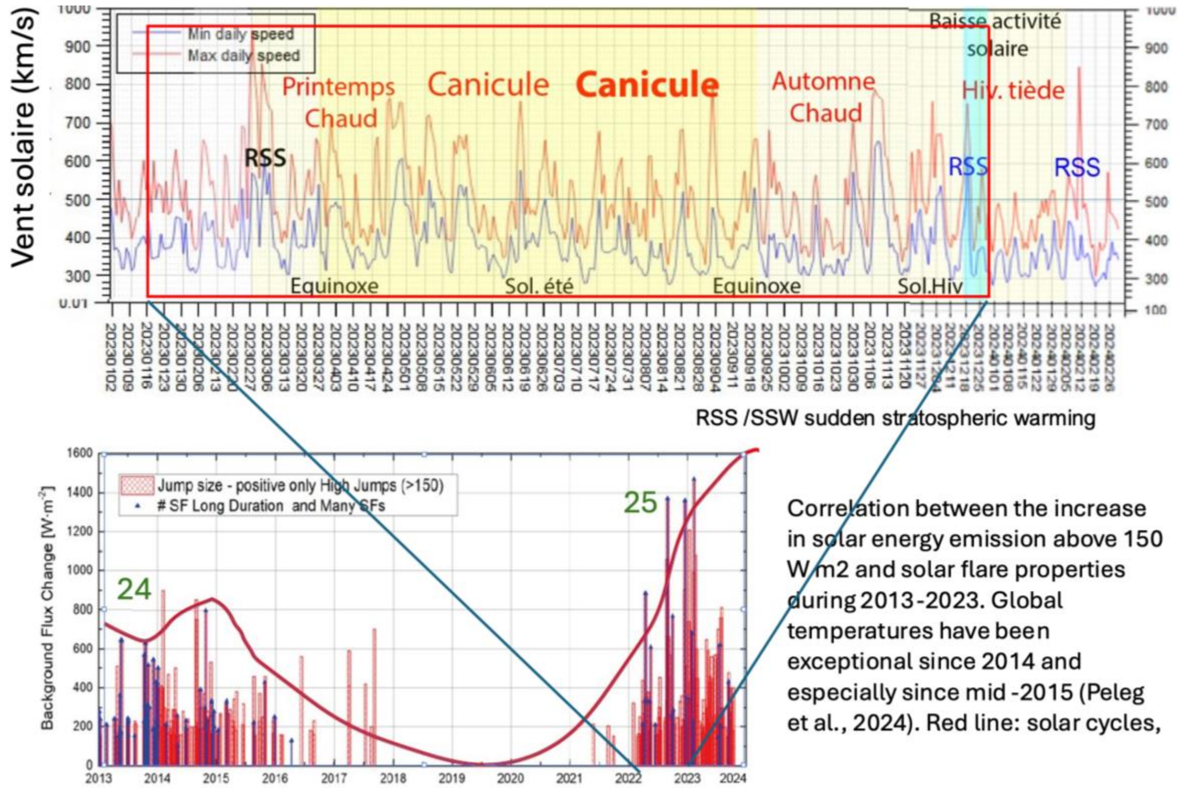

Figure 8. Correlation between heatwaves and solar activity 25/122022 01/24 (top). Below, the relationship between the frequency of coronal ejections (see also fig.4B) and solar cycles.

4.3. THE CLIMATIC PHENOMENON EL NIÑO - EL NIÑA

For the last ten years or so, EL NIÑO has been the main culprit behind the climate "upheaval" (or rather meteo-climatic phenomenon) that we have been experiencing, particularly since 2023. This aspect is attributed in the media to the increase in greenhouse gases and more particularly CO_2,

Our planet's climate is affected by the El Niño phenomenon and its counterpart La Niña, which have a lasting influence on global weather patterns for just one or two years. El Niño and La Niña are the oceanic components, while the Southern Oscillation, ENSO, is the atmospheric counterpart and is a large-scale meteorological phenomenon characterised by fluctuations in ocean temperature in the central and eastern equatorial Pacific, as well as changes in the overlying atmosphere (Domeisen, et al, 2019). We have just seen that the El Niño of 2016 (Fig. 6) is associated with a significant lengthening of the LOD, a signature of intense solar activity.

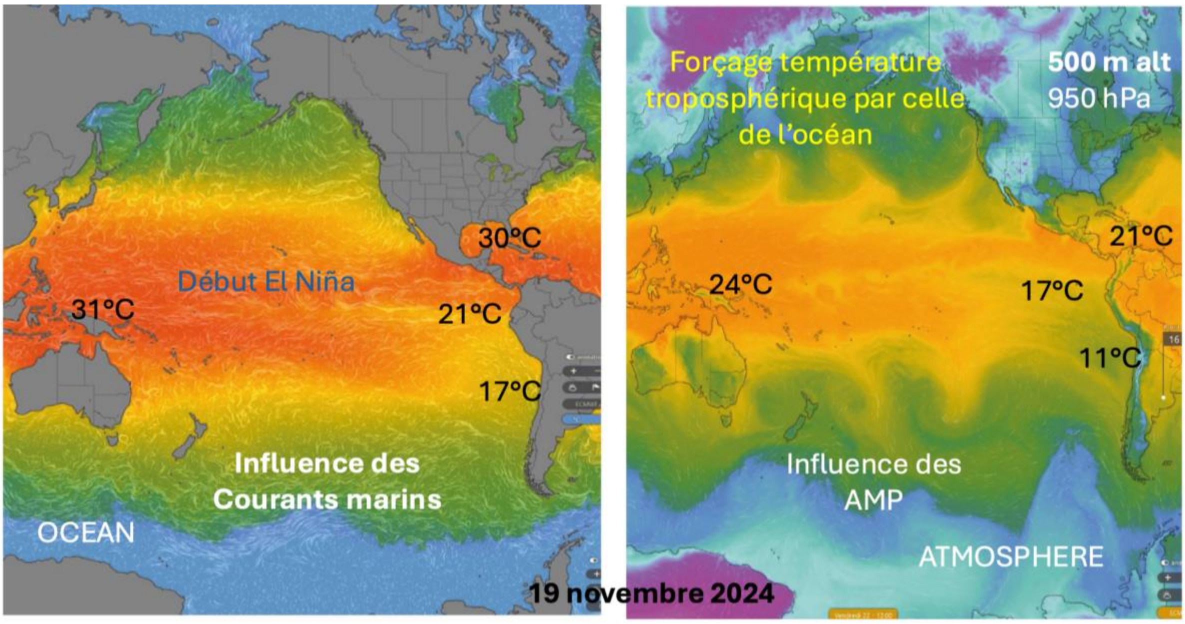

Figure 9. Comparison of ocean surface temperature with that of the lower atmosphere, which is strongly influenced by the ocean.

The Walker circulation characterises the atmospheric convective loop organised along the thermal equator over the Pacific Ocean. A slowing of the trade winds during periods of strong sunshine disrupts the Walker cycle and allows the warm, light water to spread further east along the surface of the thermocline. The westerly circulation aloft diminishes or ceases, which cuts off the supply of cold air to the eastern Pacific and the easterly surface return flow weakens. This allows the warm water accumulated in the western Pacific during the Nino to move towards South America, increasing the sea surface temperature off Peru by disrupting ocean currents. This increases cloud cover and rainfall, as well as bringing unusual temperatures to the Americas, Australia and South-East Africa. In fact, the thermal configuration of the surface and the water mass above the thermocline has a very strong influence on the tropospheric thermal configuration above it (Figs. 9 and 10). At the end of a neutral or 'normal' period, subtropical zones are colonised by cold air masses known as polar mobile anticyclones (PMAs). The same applies to sea level. We have shown that 2023 was associated with abnormal solar activity, associated with strong sudden stratospheric warming (SSR) in the northern hemisphere (SCE, [2024](#): Figure 8).

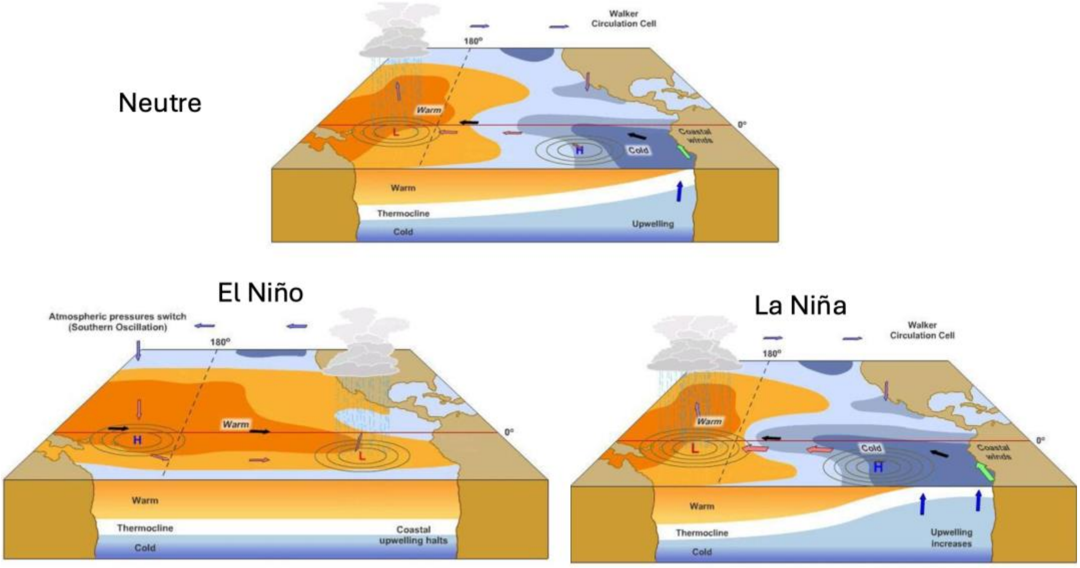

Figure 10. Temporal evolution of water masses pushed by powerful trade winds (El Niña) or spreading of warm oceanic surface waters during periods of slowing trade winds. Green: wind regime, black: water mass migration, white: thermocline.

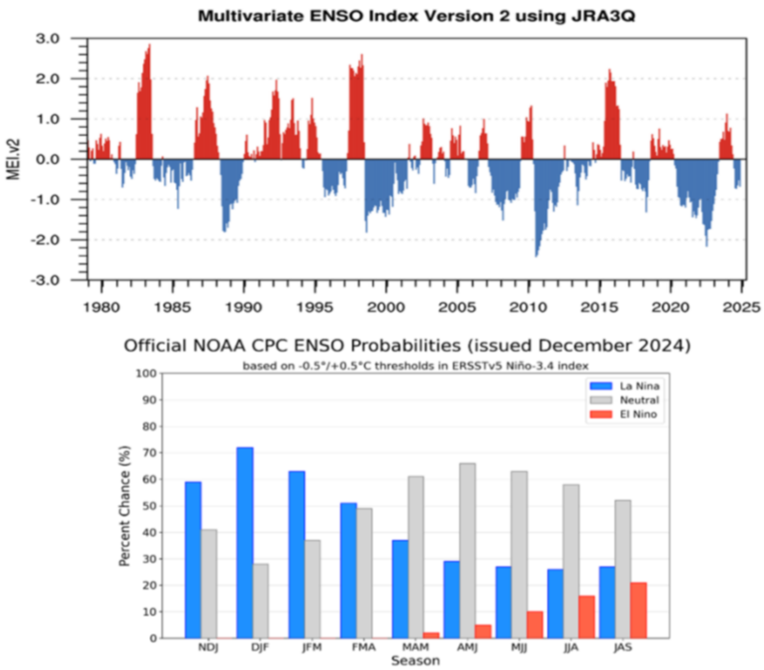

Figure 11. Evolution of El Nino countered by an increasingly powerful El Nima since 1995. NOAA forecasts for the first half of 202.5

The year 2023 brought a gradual but rapid warming of the intertropical waters, which brought an abrupt halt to a powerful Niña that had been in place since 2020 (Figure 11), coupled in 2023 with several SSRs in both hemispheres. Observations of the strength of the solar wind have shown a sudden increase in solar activity since December 2022 and a return to normal since the beginning of January 2024. We are still seeing the distal manifestations of an overheated intertropical ocean in 2024, in particular a maximum in atmospheric temperatures.

The opposite oscillation to El Niño is El Niña, which is associated with a strengthening of the Walker atmospheric cell over the Pacific and Atlantic. The strengthening of the trade winds during periods of weak sunshine (> 30km/h) stretches the area covered by the Walker cell and reinforces it. During El Niña, the strong trade winds (weak sun) push the cooler, heavier surface waters formed in the central Pacific westwards, causing the thermocline to sink progressively westwards (white band in Figure 9), which is compensated by the volume of cold water coming from Antarctica or the Arctic (Humbold and California currents) and by that which rises to the surface as a result of the exacerbation of the Peruvian upwelling (deep cold water). In fact, this replacement is also accentuated by the descent in latitude of AMPs from the Antarctic zone. In the Atlantic, the influx of cold water favours the Benguela Current off the Namib Desert, which flows up the coast of Angola before extending into the southern tropical Atlantic. In fact, on a larger scale, the El Niña functions as a mega-upwelling induced by the trade winds, leading to anticyclonic conditions and upwellings along the coasts of America (Peru and California) as also West Africa (the Namib Desert and southern Morocco), resulting in long periods of drought in these regions.

4.4. EL NINO AND HURRICANES

This year, which follows a persistent La Niña from 2021 to the end of 2023, then a long period of neutrality from March 2024, after a brief but powerful El Niño episode (July to Dec./2024) induced by the exceptional solar activity of 2023 (Fig. 8), has just returned to a Niña regime (Fig. 11). The El Niño thermal anomalies are the direct result of solar heating of the ocean coupled with a slowing of the trade winds, a strong disturbance of the tropical jet streams where most hurricanes form (Fig. 11B) and an inversion of the jet streams in the lower stratosphere, generating convective thermal anomalies over the surface and subsurface waters of the equatorial Pacific and the Indian Ocean. This also occurs, to a lesser extent, in the central Atlantic, feeding the Gulf Stream. They lead to abnormally high average temperatures during the years affected by these episodes. The trajectories of hurricanes are thus modified, including in the Atlantic. Around 0.1% of tropical convection systems can penetrate above 5,000 m, above the zone of influence of the trade winds, sometimes up to >30 km in altitude, as can volcanic eruptions.

These storms are associated with exacerbated cyclonic activity in late summer over the whole of the intertropical Pacific and the Atlantic oceans, when the waters are warmest (HN & HS). Hurricanes are not more frequent, but their power is increased for this reason, as is the convective vapour agitation over the intertropical ocean. This was the case at the end of February 2010 with the ascent of tropical cyclone Xynthia, which nucleated off the Zaire estuary, first bypassing the Azores and then raging over western France. This was also the case in 1998, a year that followed a powerful El Niño episode, associated with particularly high solar activity, as in 2023, but also responsible in Europe for flooding towards 50°N. Cyclone Chido the 14 December 2024 (summer HS) is linked to the exceptionally powerful thermal build-up in 2023, with an anomalous path around Madagascar to the north, with powerful trade winds (>20: 27 to 42 km/h) heralding a return to El Niña over the Pacific and cooling. With this warming, cyclonic storms are even moving up as far North as Alaska: they are associated with an upwelling of subtropical air in contact with descending polar air (AMP or polar mobile anticyclones, (SCE, 2022; SCE 2023) which are becoming increasingly frequent at high N or S latitudes (tongues of warm air moving polewards). In the Arctic, these have the effect of destroying the foot ice (pack ice), allowing erosion and local melting of the permafrost or, as in Spitsbergen in April 1992, freeing the Ny Ålesund fjord of ice very early in season.

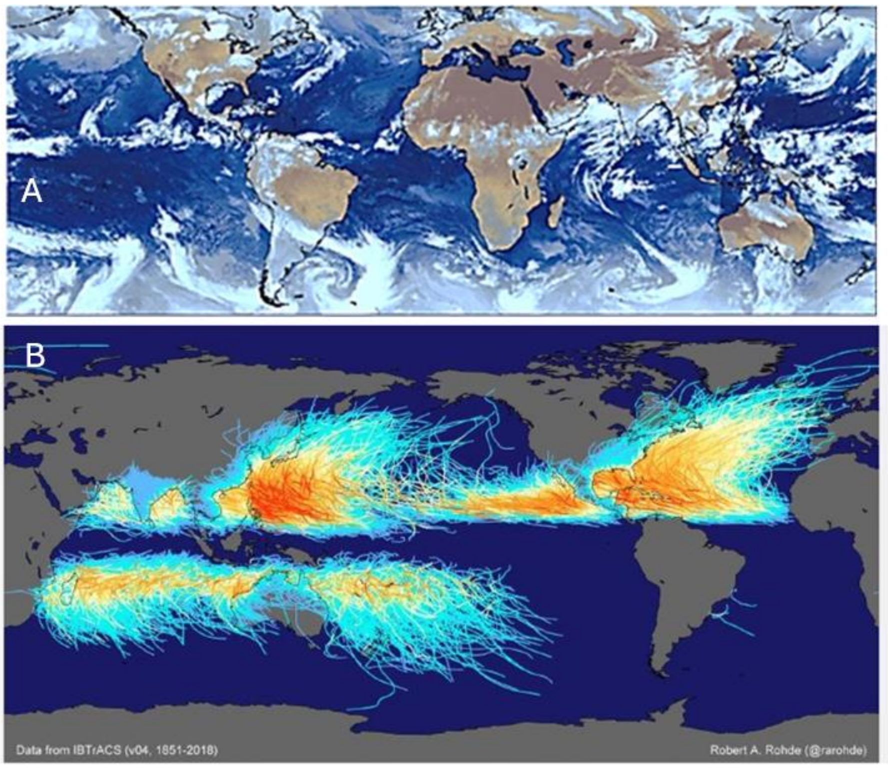

*Figure 12. Exacerbated cyclonic activity over the whole of the intertropical Pacific, but also the Atlantic, especially in late summer in HN. **A**) Composite IR satellite image taken from geostationary satellites showing the storm zone over ICTZ, slightly more spread out over Indonesia (24/06/2007 www.satmos.meteo.fr). **B**) Trajectory and power of cyclones from 1851-2018: violent phenomena are in red (R. Rohde, 2018). Note the predominance of the N hemisphere (https://x.com/RARohde/status/1011716974626443264).*

Powerful stream jets exist in the stratosphere on either side of the ICTZ, blowing at more than 100 kilometres per hour and reversing direction every 28-29 months, the QBO or quasi-biennial oscillation, wrongly attributed to El Niño. This atypical inversion is thought to emerge from chaotic processes active in the atmosphere at lower altitudes, in this case tropical storms and therefore a consequence of heat storage in the surface ocean. These cause disturbances of all sizes, known as gravity waves, which propagate around the planet during periods of active sun, just like El Niño . These warm events occur throughout the Holocene (Bond events), but more particularly during the warm events after the Holocene optimum (Moy et al., 2002).

4.5. IS CO_2 IN EQUILIBRIUM WITH THE OCEAN?

CO_2 is a gas that is soluble in water as a function of temperature. It is therefore much more soluble in cold water, i.e. near the poles, such as in the Arctic Ocean or the Peri-Antarctic, moderately acidifying the water until it is in equilibrium with the dissolved carbonates. This region is therefore a CO_2 sink. In the polar regions, the carbonate compensation depth, or CCD, corresponds to the depth below which all the calcium carbonates brought from the surface is dissolved. Below the CCD, the sediments are essentially siliceous. It is therefore logical in cold periods to have a CCD close to the surface in the Arctic (-200 m south of Banks Island), a depth above which the carbonates (foraminifera, shells) are preserved. The current CCD is between 3,000 m and 5,500 m deep in intertropical regions, allowing secondary carbonates (corals) to precipitate in the surface zone.

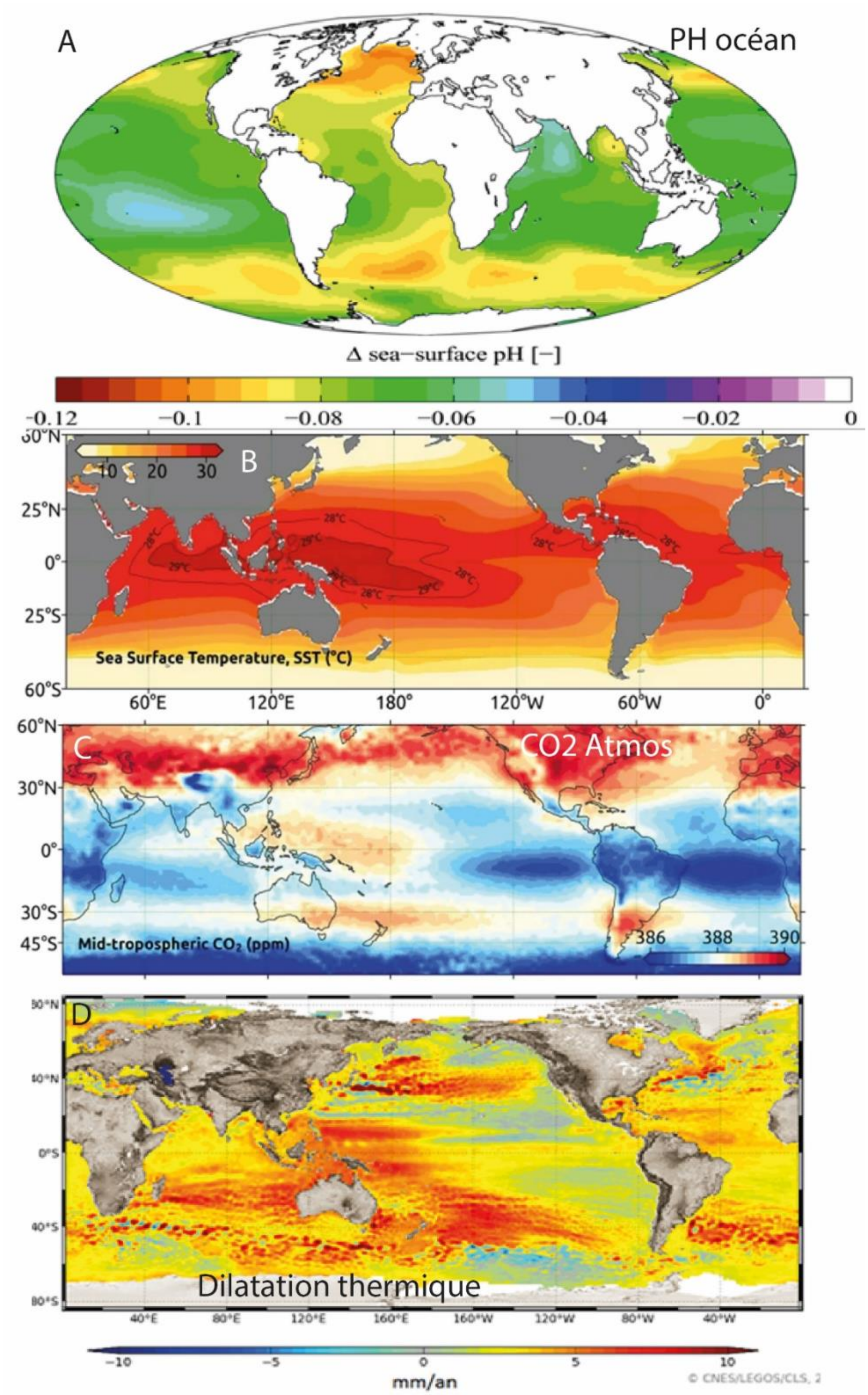

Figure 13. Breakdown of the various factors discussed in this section. ***A****) Ocean acidification between 1700 AD-1990. especially marked where CO_2 is dissolved (cold waters) (What is Ocean Acidification? - NOAA).* ***B****) Ocean surface temperature for the period 2002-2017 (Peter et al., 2023)* ***C****) Tropospheric CO_2 emitted (satellites): period 2002-2017 (Peter et al., 2023.)* ***D)*** *Ocean thermal expansion between 1993-2016 (CNES/LEGOS)*

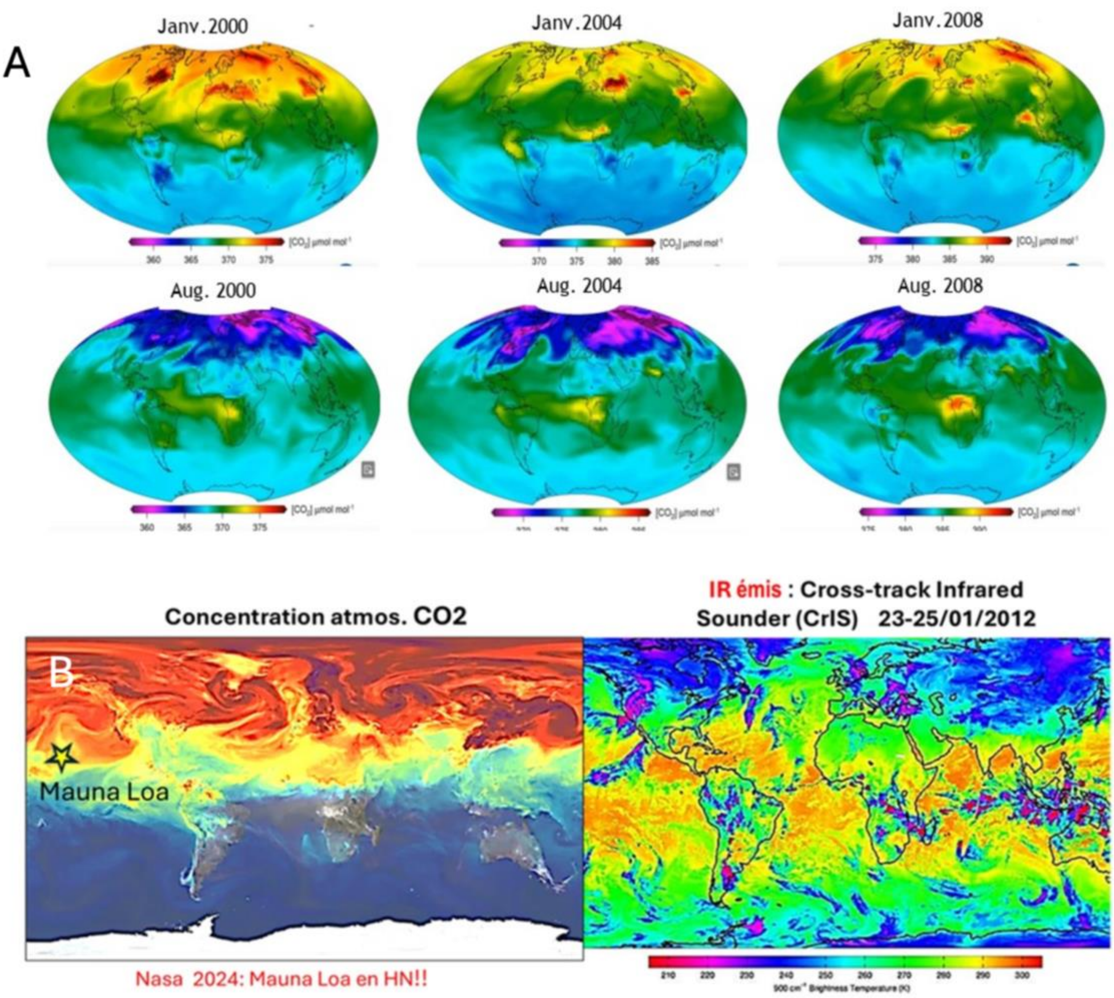

Figure 14. ***A)*** *Atmospheric CO_2 distribution by latitude in winter and summer HN. The effect of the "wall" of wind above the ITCZ is clearly visible, but penetrates the HS below moderately in winter. In the HN, the maximum concentration is regularly reached in March.* *https://www.youtube.com/watch?v=j1ehcjjDPy8&ab_channel=CarbonTracker* ***B)*** *Current distribution of CO_2 in the lower troposphere:* ***the Mauna Loa site, by virtue of its latitude (19° 28'N) and altitude (3,397 m), is not representative of the CO_2 content of the Earth's lower troposphere. Infrared re-emission logically occurs where the ocean is overheated.***

CO_2 uptake by the major oceans is modulated by marine heat waves (El Niño): the intertropical zone releases 10% more CO_2 than HN (Mignot et al., 2021; Peter et al., 2023). Deep cold currents therefore carry an excess of non-carbonate ions, which fertilise surface waters in the event of upwelling (upwelling of deep waters to leeward). In contrast, in the shallow intertropical ocean, where it is warmed by short-wave solar radiation, the CO_2 loses its carbonic acid form and is re-emitted in gaseous form towards the troposphere. The images obtained by the satellites show a strong hemispheric asymmetry in the distribution and evolution of the CO2 content of the atmosphere. Land represents 38% of the NH, compared with 18% for the HS, which is essentially oceanic. Most of the world's vegetation cover is in the Northern Hemisphere, while most of the world's population lives in Eurasia to the north of 30°N. Given the wind regime in the troposphere, there is little exchange between the 2 hemispheres, despite atmospheric convection and zonal winds. The ICTZ is a low-permeability barrier for planetary homogenisation. So, the warming of the intertropical ocean and then of the lower troposphere is directly related to solar UV activity.

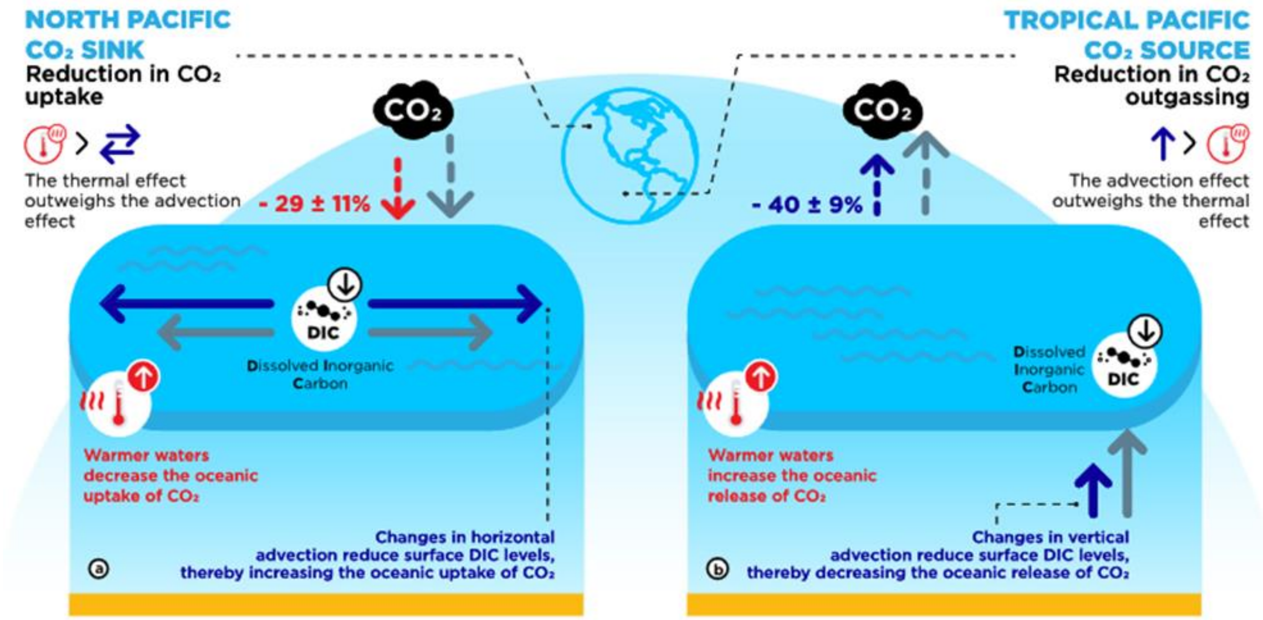

Figure 15. Mechanisms leading to a reduction in the flux of CO2 into the air in the Pacific during El Niño events: the absorption of CO2 by the large oceans at mid and high latitudes counterbalances the release of CO2 in the tropics, which is modulated by marine heatwave events (El Niño, Mignot et al., 2021;

The anthropogenic increase in CO_2 does exist, but it is modest and absorbed mainly in the northern hemisphere and has little or no influence on the global thermal balance and tropospheric temperatures.

5. WHAT SHOULD FOLLOW ?

Significant solar activity is unlikely to have ended. Similar but much more powerful events were observed at the beginning of the Bölling period (14300 BP, Bard et al., 2023) and at the beginning of the Holocene (12300BP). The coming year (2025) is not only related to the maximum of Schwabe cycle 25 but should coincide with the maximum of the Hale solar magnetic cycle that began in 2019 (CO_2 responding to a reversal of the solar magnetic field every 2 cycles to 11 years). This implies very strong solar activity like that of 2023, with the formation of large coronal holes and possible sudden stratospheric warming, which could lead to a second thermal maximum of the 21st century. This should lead to more precipitation and the release of CO_2, which would benefit the entire biological sphere, including humans.

As we have just seen, CO_2 is not a sufficient supplier of thermal energy compared to the sun, to explain the extent of the thermal phenomena observed: the release of gaseous CO_2 at the level of the ICTZ is relatively low, but already greater than what dissolves in the Northern Pacific Ocean (Mignot et al., 2021; Peter et al., 2023) . The East Antarctic ice cap will not melt and will not cause a catastrophic rise in sea level due to its thermal isolation (SCE, 2023). Using the Mauna Loa site as a reference for CO_2 levels is an aberration, given its location.

In the summer of 1859, the most powerful solar flare ever documented, known as the 'Carrington Event', struck the Earth, shattering the Earth's magnetic field and causing spectacular auroras at low latitudes. This solar coronal outburst would have been three times more intense than that of May 2024 (1200 km/sec). Such a phenomenon occurs on average every 150 years, which indicates that an eruption of this magnitude could be imminent, but our civilisation has become in 2024 highly sensitive to such effects, particularly for everything concerning electricity supply, communications and especially satellites.

Mankind is presumptuous of to believe that he can modify the climate by releasing CO2 because of his activities in the face of a simply variable star, especially as CO2 does not behave as a real GHG (SCE, 2018), unlike water vapour, which is increasing sharply in our troposphere as a result of solar activity.

BIBLIOGRAPHICAL REFERENCES

Bard E, Miramont C, Capano M, Guibal F, et al. 2023 A radiocarbon spike at 14 300 cal yr BP in subfossil trees provides the impulse response function of the global carbon cycle during the Late Glacial. Phil.Trans. R. Soc. A 381 : 20220206. https://doi.org/10.1098/rsta.2022.0206

Beggan C. D., Clarke E., Lawrence E., Eaton E., et al. 2024. Digitized continuous magnetic recordings for the august/september 1859 storms from London, UK. Space Weather 22, 3 e2023SW003807. https://doi.org/10.1029/2023SW003807

Bernhard, G.H., Bais, A.F., Aucamp, P.J. et al. 2023. Stratospheric ozone, UV radiation, and climate interactions. Photochem Photobiol Sci 22, 937–989. https://doi.org/10.1007/s43630-023-00371-y

Bizouard, C., 2017. Rotation de la Terre et IERS (International Earth Rotation and Reference System Service) https://first-tf.fr/wp-content/uploads/2017/09/2-1-50-ans-Seconde-Bizouard.pdf

Domeisen, D. I., Butler, A. H., Charlton-Perez, A, et al. 2019. The role of the stratosphere in subseasonal to seasonal prediction. Part I: Predictability of the stratosphere. J.Geophys.Res.Atmospheres, 124. https://doi.org/10.1029/2019JD030920

Ermolli I., Matthes K., Dudok T., de Wit, et al.2013 Recent variability of the solar spectral irradiance and its impact on climate modelling. Solar and Stellar Astrophysics 12 (9) 24557–24642 https://doi.org/10.5194/acp-13-3945-2013

Fronval, T., Jansen, E., Haflidason, H., Sejrup, H.P., 1998. Variability in surface and deep water conditions in the Nordic Seas during the last interglacial period. Quat. Sci. Rev., 17, 963–985. DOI:10.1016/S0277-3791(98)00038-9

Haigh, J., Winning, A., Toumi, R. et al2010. An influence of solar spectral variations on radiative forcing of climate. Nature 467, 696–699. https://doi.org/10.1038/nature09426

Lapointe F.&Bradley R.S. 2021 Little Ice Age abruptly triggered by intrusion of Atlantic waters into the Nordic Seas .Science Advances l 7, 51 DOI: 10.1126/sciadv.abi8230

Le Mouël J-L, Gibert D, Courtillot V., et al. 2023 , On the external forcing of global eruptive activity in the past 300 years. Front. Earth Sci. 11:1254855. doi : 10.3389/feart.2023.1254855

Link F. 1961 La rotation terrestre et l 'activité solaire . Czechoslovak Academy of Sciences Short communication, Bulletin of the Astronomical Institute of Czechoslovakia, vol. 12, p.70-71 .Bibliographic Code: 1961BAICz1270L

Mignot, A., von Schuckmann, K., Landschützer, P. et al. 2022.Decrease in air-sea CO2 fluxes caused by persistent marine heatwaves. Nat Commun 13, 4300. https://doi.org/10.1038/s41467-022-31983-0

Moy, C., Seltzer, G., Rodbell, D. et al. 2002. Variability of El Niño/ Southern Oscillation activity at millennial timescales during the Holocene epoch. Nature 420, 162–165). https://doi.org/10.1038/nature0119

Nikolov, N.& Zeller, K.F. 2024 .Roles of Earth's Albedo Variations and Top-of-the-Atmosphere Energy Imbalance in Recent Warming: New Insights from Satellite and Surface Observations. Geomatics, 4, 311–341. https://doi.org/10.3390/geomatics4030017

Owens, M., Lockwood, M. ,Riley, P. Global solar wind variations over the last four centuries. Sci Rep 7, 41548 (2017). https://doi.org/10.1038/srep41548

Peleg, Y. , Babayew, R. and Orion, I. (2024) The Dependence between Solar Flare Emergence and the Average Background Solar X-Ray Flux Emission. *International Journal of Astronomy and Astrophysics*, **14**, 149-161. doi: 10.4236/ijaa.2024.143009.

Ramaswamy V., Chanin M.-L., Angell J., et al. 2001 Stratospheric temperature trends: Observations and model simulations Reviews of Geophysics 39, 71-122 https://doi.org/10.1029/1999RG000065

Storini, M. 1998 Aspects of solar activity derived from interplanetary/terrestrial data Journal: Memorie della Società Astronomia Italiana, Vol. 69, p.729

Strong K, Saba J., Kucera T. 2012 Understanding space weather: the sun as a variable star Bull.Amer. Meteo. Soc. 13281335 DOI:10.1175/BAMS-D-11-00179.1

Talagrand,0. 2023. Rotation terrestre et mouvements atmosphériques », Bibnum [En ligne], Sciences de la Terre, mis en ligne le 01 septembre 2013, consulté le 04 février 2023. URL: http://journals.openedition.org/bibnum/904 ; DOI : https://doi.org/10.4000/bibnum.904

Vahrenholt F., Luning S.2015. The Neglected Sun: Why the Sun Precludes Climate Catastrophe The Heartland Institute 412 P;

Van Vliet Jean 2019 Recent-global-heat-waves-are-correlated-to-an-exceptional-solar-cycle-24 https://www.science-climat-energie.be/2019/09/05/recent-global-heat-waves-are-correlated-to-an-exceptional-solar-cycle-24/

Van Vliet-Lanoë,B. 2018, Le réchauffement climatique actuel : une évolution thermique naturelle au forçage oublié. Mythes et Mancies https://mythesmanciesetmathematiques.wordpress.com/2018/03/05/

Van Vliet-Lanoë, B., Schneider, J.L., Guðmundsson, Á., Guillou, H., Nomade, S., Chazot, G., Liorziou, C., Guégan, S., 2018. Eemian estuarine record forced by glacio-isostasy (S Iceland) - link with Greenland and deep sea records. Can. J. Earth Sc, 55:(2), 154 - 171, 10.1139/cjes-2017-0126

Voosen P. 2024. El Niño fingered as likely culprit in record 2023 temperatures suggests swings in Pacific Ocean can account for planet's sudden and perplexing temperature jump. Science 386, 6718,137 . DOI: 10.1126/science.adt7207

White, W. B., Dettinger M. D., Cayan D. R., 2003 Sources of global warming of the upper ocean on decadal period scales, J. Geophys. Res., 108(C8), 3248, doi:10.1029/2002JC001396, 2003..

Xie, F., Xia, Y., Feng, W. et al. Increasing Surface UV Radiation in the Tropics and Northern Mid-Latitudes due to Ozone Depletion after 2010. Adv. Atmos. Sci. 40, 1833–1843 (2023). https://doi.org/10.1007/s00376-023-2354-9